Radiation environment and its effects on the Martian surface and underground

Pedro Magalhães
pedro.m.magalhaes@tecnico.ulisboa.pt

Instituto Superior Técnico, Lisboa, Portugal

April 2016

Abstract

Since a long time ago, human civilization dreams about making a journey to Mars, both for gradual exploitation of the Solar system and to defy the human limits.
Among all the discoveries that humankind made from this planet, there is one that excels, which is the presence of liquid water that may still be conserved. Water is vital to life as we know it, so the presence of water increases the likelihood of Mars having or having had life on its surface or subsurface. Astrobiology is the study of the origin, evolution, distribution and future of life in the universe, incorporating the pursuit of habitable environments either within our Solar System or outside. Therefore, the study of Mars' radiation evironment and explotation of the possibility of life under such conditions appears as a natural topic for this Master thesis since it is a direct application of this branch of Physics to a mission that is still being planned and evaluated to our nearest neighbour planet. The work in this thesis includes the simulation and study of the radiation environment, both at the surface and at different depths of the subsurface, in order to analyze the implications for the formation and evolution of life. This was achieved using Geant4, which stands for Geometry and Tracking, and it is a toolkit for simulation of the passage of particles through matter, using Monte Carlo methods and developed at CERN, which is freely available from the project web site.
Keywords: Mars, Radiation, Astrobiology, LET, dMEREM.

1. Introduction

The continuous development of simulation tools, namely to predict the radiation field in both free space and on planetary surfaces, is extremely important for the planning of a manned mission to Mars, and to other planets as well.
Mars Exploration Program is a NASA program which aims to discover if Mars is potentially a habitable planet and to study the geophysical processes that were responsible for its formation and evolution to the planet as it is now. Curiosity is the largest planetary rover ever sent to Mars, with a mass of approximately 900 kg, 2.9m by 2.7m and 2.2m tall, is part of NASA's Mars Science Laboratory mission. It all began at August 7th, 2012, when the Curiosity rover landed on Mars at the Gale Crater site .[1] This was the first day in the history of mankind that measurements of cosmic rays and solar energetic particles at Mars' surface took place. These measurements occurred over 300 days during the maximum solar activity, not only at Mars' surface, but also during the ship's trip from Earth, with the Mars Science laboratory installed in its the interior.

1.1. Radiation in Mars

The radiation environment in space is a complex mixture of energetic charged particles that poses a major health concern for astronauts on long-duration missions. The space radiation environment consists of three broad categories (National Council on Radiation Protection and Measurements, 1989, 2000), which are trapped particle radiation, solar particle radiation and galactic cosmic radiation (GCR), with protons being the most abundant particle type.
Since Mars lacks a global magnetic field, its radiation environment is mostly constituted by both Galactic Cosmic Rays and Solar Energetic Particles, which affect the evolution of the climate of Mars, the operation of satellites, and the human exploration of the planet [7].

1.1.1 GCR

According to the ICRU (International Comission on Radiation Units & Measurements), cosmic ra-

[1] a Crater on Mars, located at the Northwestern part of the Aeolis quadrangle at 5.4°S 137.8°E.

diation is the ionizing radiation consisting of high energetic particles, primarily nuclei of extraterrestrial origin, and the particles they generate due to their interaction with an atmosphere and other crossed matter [12]. These nuclei are originated mostly within our galaxy, but outside our solar system. It is important to note that this radiation, while entering Mars' atmosphere, produces secondary particles, even though its density is approximately 1% of the Earth's atmosphere. So, taken into account its origin, it is natural to comprehend that it is essentially an isotropic radiation Although every natural chemical element is part of this radiation, around 87% are protons and roughly 12% are alpha particles. These particles are predominantly accelerated in the Milky Way. At very high energies, the particles are actually assumed to be originated from powerful astrophysical accelerators, such as supernova explosions or quasars, located outside of the Milky Way [2].

Their flux is influenced by the background level of solar activity, thus having seasonal effects. At higher solar activity level, lower energy particles from the incident radiation will be removed, due to the complex interplanetary magnetic fields [10], thus decreasing its flux. This effect is known as solar modulation effect and it can be seen in Figures 1.1.1 and 2, which shows the GCR differential flux spectrum at solar activity minimum and maximum, respectively, at the Solar Cycle 23 for hydrogen, helium, lithium and iron nuclei [9].

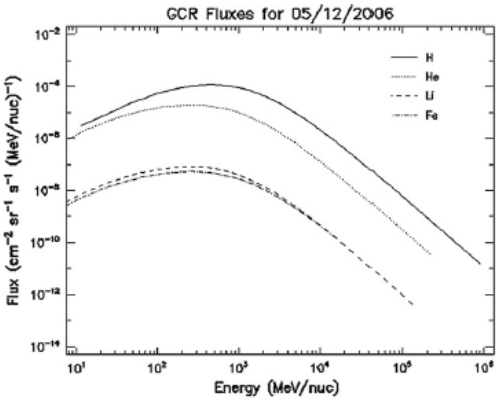

Figure 1: Differential GCR flux spectrum as a function of energy at solar minimum for solar cycle 23 [10].

For energies higher than 1 GeV, the solar modulation effect is not quite relevant. Although cosmic rays' energy may reach values up to 10^{20} eV, as can be seen in figure 3, most of its hazardous effects are associated within the range of nuclei with energies between several hundred MeV and a few GeV (Guetersloh et al., 2011), since the flux dicreases exponentially with energy. The interactions of these particles with the Martian atmosphere produce a large amount of secondary particles, which themselves may also produce further cascades of extra secondary particles, giving rise to a high particle flux.

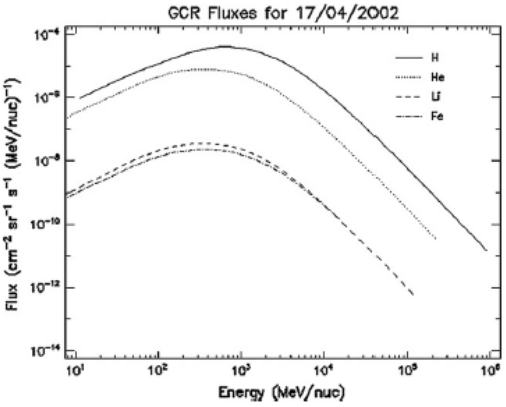

Figure 2: Differential GCR flux spectrum as a function of energy at solar maximum for solar cycle 23 [10].

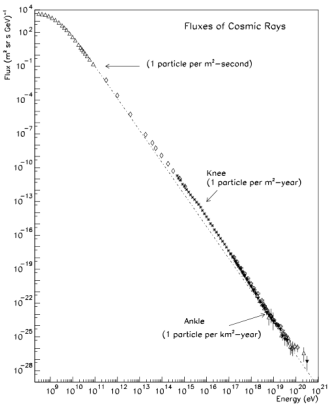

Figure 3: GCR energy spectrum [13].

Because of their high energies, GCR are difficult to shield against and can penetrate a few meters into the martian soil [8], as will be studied in this thesis.

1.1.2 SEP

Solar flares and coronal mass ejections are the source of these particles, existing a correlation between the flux of these particles and the solar activity, namely the occurrence of a solar eruption. They are mostly composed of protons, with the remaining being around 10% He and less than 1% heavier elements [10], and can be highly accelerated, having energies up to some GeV per nucleon. The detection of solar neutrons is quite rare, since their half lifetime is around 11.7 minutes, so most

of them already decayed before reaching Mars and Earths surface.
SEP events are sporadic and their flux may vary by several orders of magnitude, hence difficult to predict, with durations that spans from a few hours to days. SEP with energy higher than 10 MeV per nucleon are considered hazardous to personnel involved in extravehicular activity at the surface of Mars [10]. Protons, regardless of being GCR or SEP descendant, with a kinetic energy less than $\simeq 150$ MeV shall not be able to reach the surface, assuming an atmospheric depth column of 20g/cm^{-2} [8].

1.2. Radiation quantities

1.2.1 Linear Energy Transfer

The linear energy transfer, LET, is defined as the energy deposited by an ionizing particle in matter per unit length of its trajectory (dE/dx), so it is measured in J/m. Division by the absorbing mediums density allows the LET to be density-independant, so the LET profile does not change much from medium to medium. There are two types of linear energy transfer: collision and radiative. The former outcomes from the interaction of the incident radiation with the atomic orbital electrons of the medium, while the latter results from the interaction of charged particles with the atomic nuclei, causing them to change their direction and acceleration. These particles will then, in this latter situation, radiate *Bremsstrahlung* photons.
The energy losses by a charged particle while interacting with the medium, where quantum mechanics is taken into account, was firstly computed by Bethe and Bloch (1932).

1.3. Biological effects of radiation

Ionizing radiation may have biological effects, ergo affecting human life, whether the source comes from therapeutic and medical diagnosis or it is a natural resource, and whether it is a small or large dose of radiation.
There are two major classes in which radiation can affect the cells, which are called the direct and indirect effects. It is referred to as a direct effect, any radiation that interacts with the DNA molecules atoms or some other structure critical to the survival and to the normal function of the cell. When a cell is exposed to radiation, the probability that it actually interacts with the DNA molecule is very small, due to the fact that the cross section of this interaction is very small, since these critical components occupy a really small part of the cell, which is mostly composed by water. Therefore, it is highly likely that the radiation will interact only with the water in the cell. When this happens, the radiation may break the chemical bonds that hold the water together, producing hydrogen (H) and hydroxyls (OH). These fragments will likely interact with other ones, with ions or even with one another, forming compounds, such as water, thus not harming the cell. However, they may also combine to form toxic substances, such as hydrogen peroxide (H_2O_2), which can contribute to the cells destruction. This is a good example of an indirect effect of radiation. It is not hard to imagine that these indirect effects, although less dangerous in general, happen more frequently than the direct ones. The direct effects are predominant for radiation with higher LET, such as neutrons, protons and alpha particles.
There are four possibilities that can occur when radiation interacts with the DNA, depicted in figure 4. The first, being the least worrying case, is when the cell completely repairs the damage inflicted by the radiation. If the damage is strong enough, the cell dies. In some occasions, the cell may resist

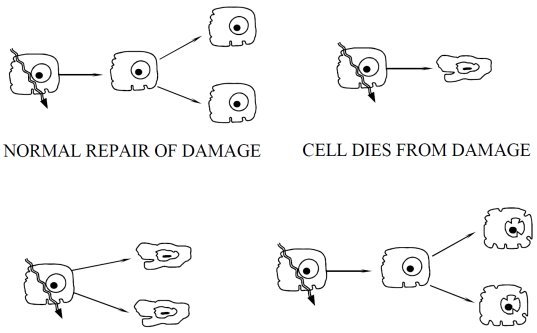

Figure 4: Sketch of possible outcomes of radiation interaction with DNA

the damage and is able to replicate itself, but the daughter cells die, due to the lack of some critical component. The last scenario, but not the least, being in fact the most dangerous of all the scenarios above, is when a cell is affected in a way that it does not die, but becomes mutated, while not losing its ability to reproduce, thus extending the mutation to its daughter cells. This could be the origin of a malign tumor, leading ultimately to cancer [3].

1.3.1 Relative Biologic Effectiveness

If one wants to make the most realistic experiment possible, one has to irradiate a sample of bacteria and estimate the survival and mutation times. It is not economically feasible, though, to generate all the different types of radiation that reaches the Martian surface, nor would be completely safe, since some quantity of radioactivity would be present. For these reasons, it is necessary to have a different and, at the same time, reasonable approach. The Relative Biologic Effectiveness (RBE) of some test

radiation **r** compared with x-rays, according to the National Bureau of Standards in 1954, is defined as being the ratio D_X/D_r, where D_X and D_r are, respectively, the doses of x-rays and the test radiation required to produce the same biological effect. In order for this quantity to make sense, one shall choose a biological system in which the effects of radiation may be evaluated quantitatively [4]. In general, the greater the RBE, the more hazardous the test radiation will be.

1.3.2 Relation between RBE and LET

RBE and LET are related quantities. Figure 5 shows the dependency of RBE with LET for mammalian cells of human origin, with the first, the second and the third curve representing survival levels of 0.8, 0.1 and 0.01, respectively. It can be seen that the RBE does not exclusively depend on the radiation, but also depends on the level of biological damage and, therefore, on the dose level [1]. One thing in common, though, is that in all three cases RBE increases slowly until 10 keV/μm, and then it starts increasing rapidly with LET, where the maximum of RBE is registered at 100 keV/μm. Beyond this value, RBE starts to decrease to lower values.

The optimal LET for biological damage is, thus,

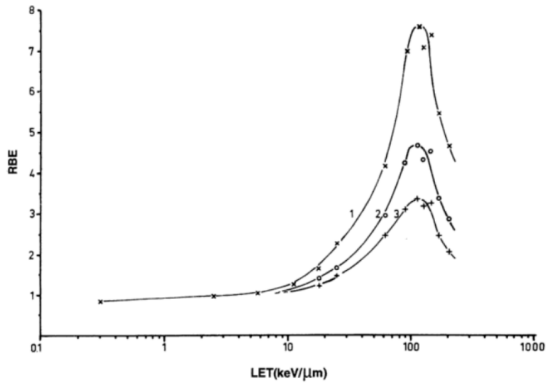

Figure 5: RBE as a function of LET for survival of mammalian cells of human origin [1].

around 100 keV/μm. This happens because, at this density of ionization, the separation of two events coincides with the diameter of the DNA double helix, which is approximately 2 nm. So, radiation which has a mean separation of events that coincides with the DNA double helix is more likely to cause double-strand breaks, hence is more hazardous to life, since the exchange-type aberration due to the interaction of two double-strand breaks is the basis of most biologic effects [4].

The current state of the art of LET at Mars is the Curiosity's measurement at the surface, which is shown in figure 6. The same figure also shows the LET measurement inside the Mars Science Laboratory (MSL) spacecraft during its journey from Earth to Mars. This LET was computed in water,

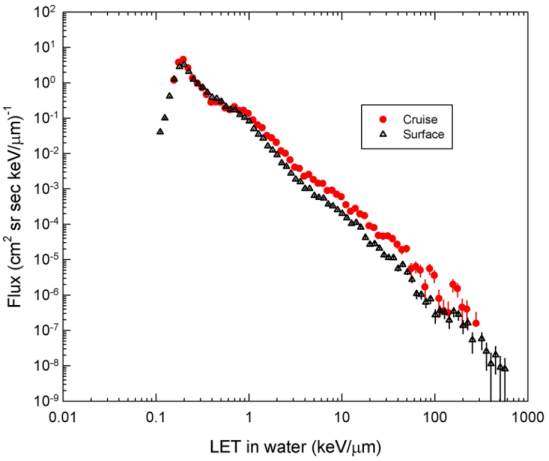

Figure 6: LET spectrum comparison between the measurement during the cruise journey inside the MSL spacecraft (red) and the surface of Mars (black) [8].

since it represents the major composition of known life. As one can see, the flux corresponding to a 100 keV/μm LET is significantly low (around 10^{-6} particles per cm^{2}sr sec keV/μm), and the majority of the LET flux is located around 0.2 keV/μm, which has an RBE value around 1.

2. Implementation

Since the damaging effects of ionizing radiation on biological structures, such as cells, is one of the greatest limiting factors on the survival of life, the aim of this thesis is to analyze the radiation environment, not only at the surface of Mars, but also at regular depths of its soil. These simulations will take place on two different scenarios, both related to weather scenarios modulated by the sun, namely at solar activity minimum and maximum. For the latter, two different kinds of radiation will be simulated: GCR, and SEP, whereas for the former only protons and α particles coming from GCR will be simulated, since the probability of having an SEP increases with solar activity. Plots of particle flux (primary and secondary particles) as a function of energy of the primary and as a function of the LET will be analyzed. This LET is calculated in water, since it represents the major component of life as we know it. All this information combined will make possible the understanding of preservation limits of organic matter in the Martian soil.

A schematic representation of all parties involved in the simulation framework is shown in figure 7.

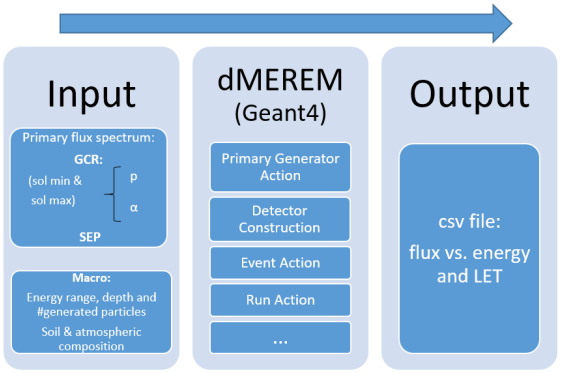

Figure 7: Representation of the simulation framework

2.1. dMEREM

The detailed Martian Energetic Radiation Environment Model (dMEREM) is a Geant4 application, which enables a Monte Carlo analysis of the Martian radiation environment, providing a high fidelity simulation, not only of the environment, but also of the physical interactions between all particles considered, such as protons, gamma radiation and heavy ions. It was developped under ESA's MarsREM Project, also involving LIP (Laboratrio de Instrumentao e Fsica Experimental de Partculas).

In this thesis, the new fixture of dMEREM is the possibility of detecting particles below the surface. The first detector is located at the surface of the Martian soil, while the last one is placed at a depth of 3 m, as depicted in figure 8, where the position of all 12 is shown. These 12 layers shall provide a good insight about the profile of the radiation environment of the Martian soil within a lower depth. dMEREM is composed by an atmosphere of 20 layers, each with its own density and composition, while maintaining the same thickness (in g/cm^2). This means that since the atmosphere's density is higher at lower altitudes, the lower layers will be thinner than the higher ones, in order to guarantee the same thickness. The atmosphere is 50 km high and the soil is 100 m deep, both 300 km wide.

2.2. Input

dMEREM receives an incident energy-flux spectrum as input, in this case by SPENVIS, which stands for Space Environment Information System. Using this webpage, the user can control the incident particle spectra, choosing which model and database to use. The SPENVIS parameter page allows the user to define the

- epoch of study;
- latitude, longitude and altitude (km above the surface) or depth (g/cm^2 below the surface);

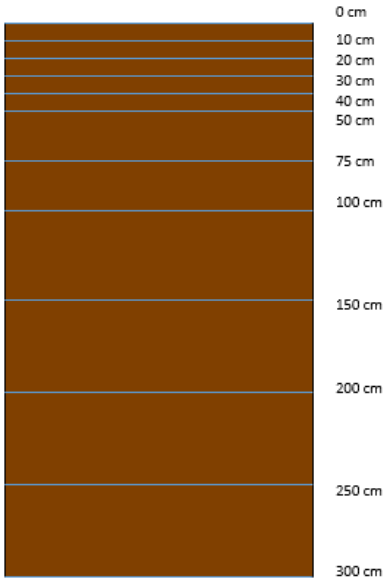

Figure 8: A sketch of the position of all detectors within the martian soil.

- area of the geometry to be used, also in km;
- soil composition and density, which can both be user defined;
- source type, where SEP, GCR or X rays can be selected;
- number of primary particles to be generated, spanning from 10^2 to 10^5;
- physics scenario, where the user can make a *quid pro quo* between simulation time and precision.

The input file to be read by dMEREM is a two-column csv file (comma-separated values), one column with the energy and the other with the flux. The conditions of how the particles are generated, as well as their type, quantity and energies are defined through a macro that is read by dMEREM just before the start of the run, which may be also provided by SPENVIS. This way the user does not have to modify anything inside dMEREM. Thus, the user is able to define the energy ranges to be generated, as long as it is contained in the input spectrum.

3. Results

Table 1 shows the conditions of generation for the different simulated scenarios, with the atmosphere and soil compositions for Gale Crater. The soil is mostly composed by SiO_2 and bulk, which is a mixture of Al_2MgCa, Na_2 and K_2O_3. The atmosphere is mostly CO_2. A cut of 100 keV on the generation of secondary particles was imposed, this means that no secondary particles with kinetic energy below that value will be created.

Table 1: Table summarizing all simulations.

Type of Radiation	Energy range	Statistics
GCR-proton (max&min)	10 MeV - 1 GeV	5M
	1 GeV - 100 GeV	500k
GCR-α (max&min)	10 MeV - 1 GeV	5M
	1 GeV - 100 GeV	250k

3.1. GCR

The input spectrum of both proton and alpha particles is presented in figure 9, for both solar minimum and maximum.

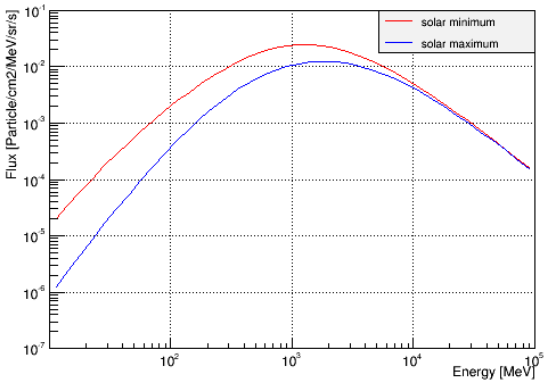

(a)

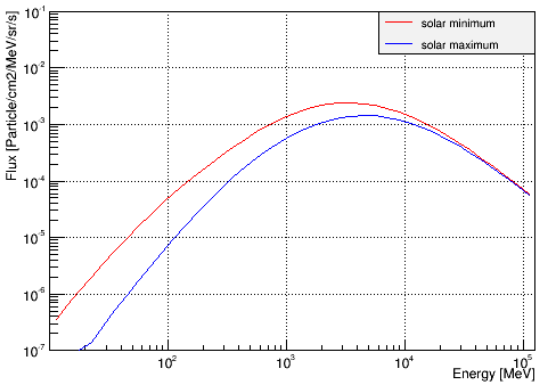

(b)

Figure 9: GCR flux spectrum as a function of energy for protons (a) and alpha particles (b), as input to dMEREM.

3.1.1 Protons

As seen in Figure 10, at the surface the flux increases until around 0.5 GeV and then it starts to decrease, presenting a similar trend of the spectrum given as input. The flux's peak is actually slightly shifted to the left (the energy of the peak is around 500 MeV, not reaching 1 GeV). Comparing the proton flux at the surface to the input spectrum, one

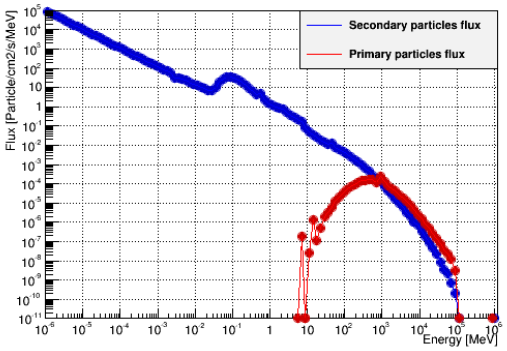

Figure 10: Primary and secondary particle flux for solar minimum, at the surface.

concludes that the Martian atmosphere is not negligible, since interactions of the primary particles with the latter are quite significant.

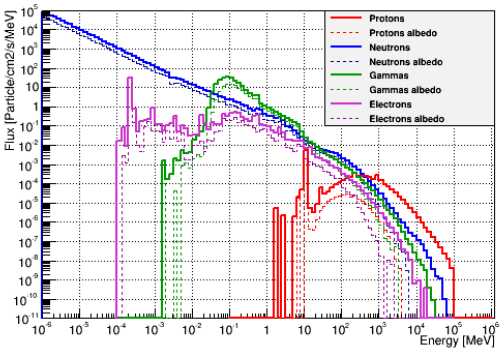

Figure 11: All particle flux for solar minimum, at the surface.

There are secondary particles with energies around the eV being created, not only in the atmosphere, but also due to interaction of the primary particles with the soil. As one can see in figure 11 at the surface, up to $\simeq$ 10 keV, the majority of these particles correspond to (thermal) neutrons. The reaction responsible for neutron production, as well as some other particles, is due to the interaction of the cosmic rays with the nuclei of the atmosphere through spallation [6]. A fast neutron (kinetic energy above 20 MeV) loses its energy mostly through elastic scatterings, where it will be slowing down. As the neutron loses its energy, it will undergo several random elastic collisions, increasing the probability of it to be captured. We also see the formation of electrons, which generate *Bremsstrahlung* photons. A direct consequence of the 100 keV cut is the increase in the flux of lower energy protons, since without the cut they would form secondary particles with energy below this threshold, thus disappearing at higher energies. The deposited energy

is the same as the no-cut scenario.
Comparing figure 9(a) with 10, one concludes that the protons reaching the surface are mostly primary particles, with the exception on energies below $\simeq 10$ MeV, clearly dominated by secondary protons generated due to the interaction radiation with the atmosphere. Figure 12 shows the particle fluxes at 3

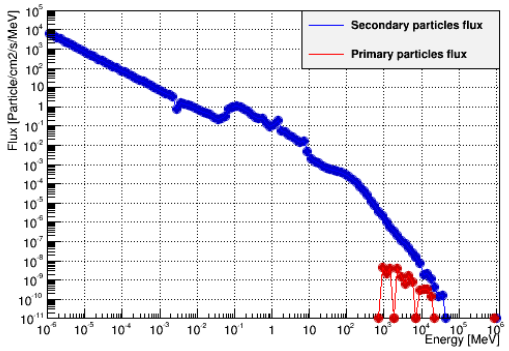

Figure 12: Primary and secondary particle flux for solar minimum, 3 m deep into the soil.

m underground, showing a decrease in the primary particles' flux. This is expected due to the increase of the shielding provided by the soil, gradually absorbing those primary protons and originating secondary particles.

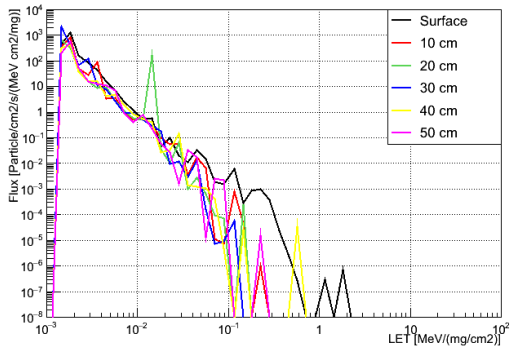

Figure 13: LET from the surface to a 50 cm depth on solar activity minimum.

To compare these LET values with their respective RBE, one must convert the presented units to keV/μm, which is rather straightforward, and is shown in equation 1.

$$\begin{aligned} & 1\text{MeV cm}^2/\text{mg} \times \rho_{H_2O} = \\ = \; & 1\text{MeV cm}^2/\text{mg} \times 10^3\text{mg/cm}^3 = \\ = \; & 10^3\text{MeV/cm} = 100\text{keV}/\mu\text{m} \end{aligned} \quad (1)$$

The worst case LET scenario corresponds to 100 keV/μm (see section 1), which corresponds to 1

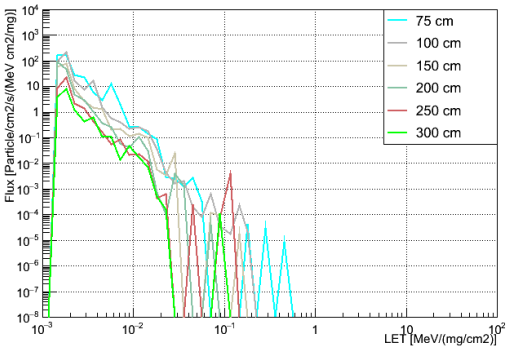

Figure 14: LET from 75 cm to 3 m on solar activity minimum.

MeV cm^2/mg. During the solar minimum, as seen in Figures 13 and 14, this value of LET has a very small contribution from the surface and down to 50 cm into the ground. At larger depths the LET never attains this value. Although the RBE maximum is reached with LET values of 1 MeV cm^2/mg, RBE starts to increase with LET values from 0.1 MeV cm^2/mg. Despite these flux values being relatively low, they are not negligible down to 250 cm underground. At 3 m LET barely reaches 0.1 MeV cm^2/mg, so the respective RBE value remains at $\simeq 1$.

3.1.2 Alpha particles

The input spectrum can be seen in Figure 9(b). Similarly to the protons, at the surface α particles'

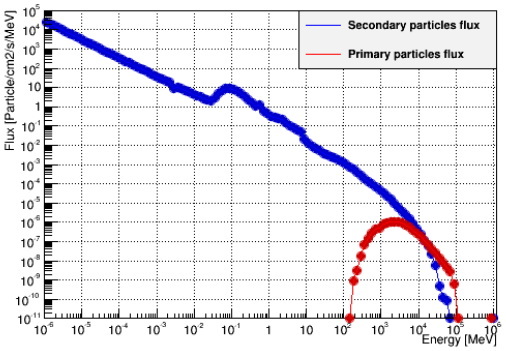

Figure 15: Primary and secondary particle flux for solar minimum, at the surface.

flux follow the trend of the input spectrum, with the flux peak being slightly shifted to the left, as one would expect, since the particles lost some of their energy traversing the atmosphere, as the Figure 15 shows. The primary particles are almost completely absorbed in the first centimeters of the soil. Since α

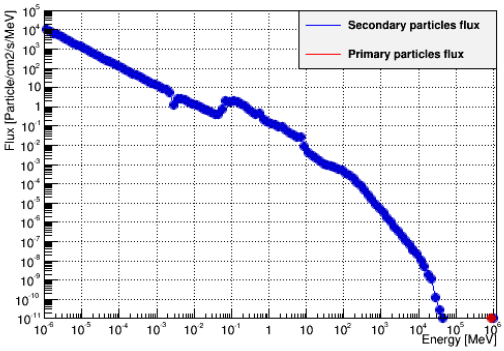

Figure 16: Primary and secondary particle flux for solar minimum, at 1.50 m deep inside the soil.

particles have twice the charge than protons, they will losing energy on an earlier stage, since, according Bethe-Bloch equation, the energy loss of a particle is proportional to its charge squared. At a depth of 1.5 m there is no primary flux. A more

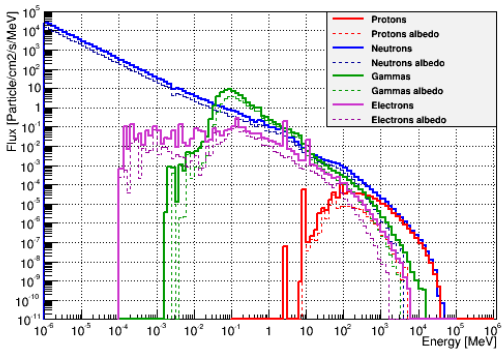

Figure 17: All particle flux for solar minimum, at the surface.

detailed view of the flux of each secondary particle is shown in figure 17. Observing Figures 18 and

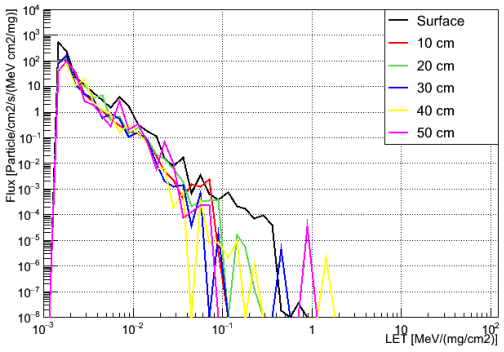

Figure 18: LET from the surface to a 50cm depth on solar activity minimum.

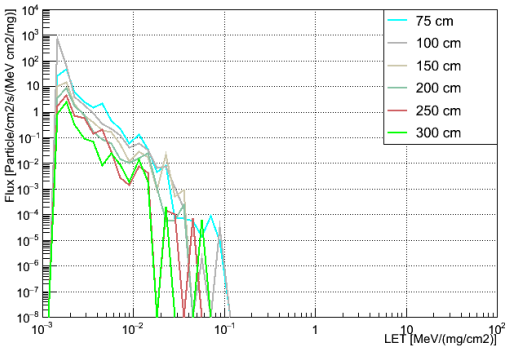

Figure 19: LET from 75 cm to 3 m on solar activity minimum.

19, and having in mind that RBE starts to increase to higher values for LET values between 0.1 MeV cm^2/mg and $\simeq$1 MeV cm^2/mg, it is possible to conclude that, for both solar activity levels, in the first 2 m of the soil, some occurrences of this hazardous LET were registered. Comparing these LET values with the proton-like GCR, the α-like GCR seems to be more hazardous, since down to a depth of $\simeq$ 2 m the LET flux between 0.1 and 10 MeV cm^2/mg is not negligible.

3.2. SEP

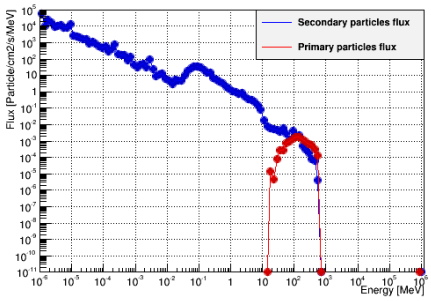

Figure 20: Primary and secondary particle flux (a) and all particles' flux (b), both at the surface.

Observing Figure 21, one concludes that after 1 m of soil depth no SEP events are detected. Looking at the full particle spectrum at the surface, Figure 21, it can be seen that the neutron flux remains dominant until $\simeq$ 10 keV, giving rise to the formation of γ. Although in a less dominant way, electrons are also formed, being responsible for the formation of that γ radiation. Observing Figure 23(a), which correspond to the first 50 cm of the soil depth, and comparing it to the LET of protons or α particles, whether on solar maximum or minimum, one concludes that SEP events have few impact or no impact at medium-high LET, since it only reaches 0.2 MeV cm^2/mg at the surface. Underground, its

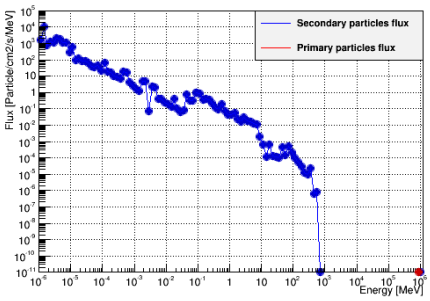

Figure 21: Primary and secondary particle flux at 1 m deep.

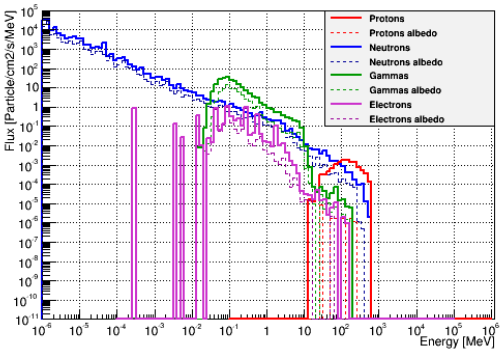

Figure 22: All particle flux for solar minimum, at the surface.

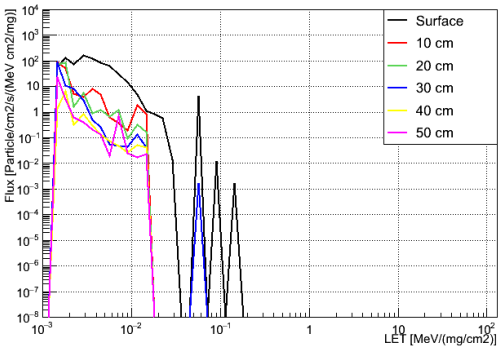

(a)

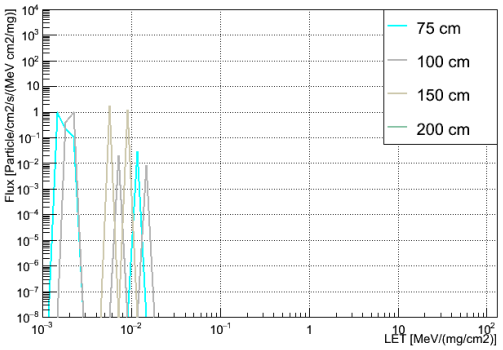

(b)

Figure 23: LET due to solar event particles at different soil depths.

values are below 0.02 MeV cm^2/mg. Looking at figure 23(b), one sees that up to 2 m deep, no traces of LET are detected.

3.3. Validation with Curiosity

Curiosity's LET measurements constitute the state of the art of the Martian surface LET, presented in figure 6. Figure 24 shows both spectra superimposed in the same graph. In both cases the flux spans across the same LET values, and the flux measured by Curiosity is comparable to the one computed by dMEREM, apart from the lower and greater values. As mentioned earlier, in the high-LET regime, few events were detected, meaning that the statistical uncertainty becomes higher, which may explain the divergence in these high-LET results along with the fact that in this thesis only protons and alpha particles were simulated. Other elements like Carbon and Oxygen are known for having a non-negligible contribution to the LET. Curiosity's detector's amplitude is smaller, since the geometry factor is 0,17 cm^{2}sr [5] with an area of 1,92 cm^2 [8], corresponding to a half field of view (FOV) angle of only 9,63° (0,1681 rad). Whereas in the case of this thesis, the simulated half FOV is 90°. This might explain the discrepancy in the low-LET region. Since the flux depends on $\cos^2(\theta)$, with θ being the particle's incident angle measured from the vertical, the flux computed by dMEREM is lower than it would have been if computed with the same FOV as Curiosity, since larger angles are taken into account.

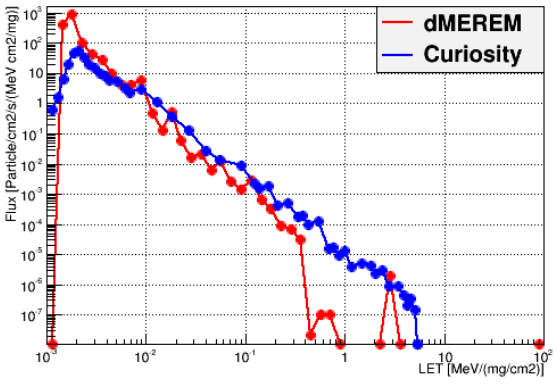

Figure 24: Comparison of Curiosity's in situ LET spectrum measurements with the one computed by dMEREM.

4. Conclusions

In the GCR case, it is possible to conclude that the protons travel farther into the Martian soil than the α particles, for the latter cease after 150 cm of regolith soil. This is somewhat expected due to their higher charge, since, according to Bethe-Bloch formula, they will lose more energy per unit length, which is corroborated by the increase in LET.

The damage in biologic materials increases with the RBE, which increases with LET from values bigger than 10 keV/μm, or 0.1 MeV cm^2/mg, according to figure 5. Non-hazardous LET is reached at $\simeq$ 150 cm depths, in the case of protons, in both solar minimum and maximum. For α particles, non-hazardous LET was registered, in solar minimum, at 75 cm, and at 1 m for solar maximum. This means that below these depths, the radiation environment is acceptable for microorganisms, since the associated RBE is $\simeq 1$. Although the low LET particles are associated with low RBE and cause little damage to the DNA, their fluxes are much higher than in the last case, going up to roughly 6 orders of magnitude over the flux registered at 10 keV/μm.

The SEP are quickly absorbed in the Martian soil, which is somewhat expected due to their low energies, when compared to the GCR. Even at the surface, the LET barely reaches the hazardous region.

The Curiosity results for the measured LET are in reasonable agreement with the ones presented in this thesis for the LET at the surface of Mars. However, there are discrepancies to be understood that may be related to the acceptance of the real detector being smaller than the simulated one (covering only a specific part of the angular distribution of the particle arriving the surface) and also the fact that in this work only protons and α particles were simulated, while heavier ions reaching the Martian surface would contribute to the higher LET region. These differences should be better understood in a future analysis.

References

[1] Barendsen. Response of cultured cells, tumours and normal tissues to radiations of different linear energy transfer. *Curr Top Radiat*, IV:293–356, 1968.

[2] C. Baumstark-Khan and R. Facius. *17- Life under Conditions of Ionizing Radiation.*

[3] US Nuclear Regulatory Commission, editor. chapter 9 - Biological effects of radiation.

[4] Amato J Giaccia Eric J Hall. Radiobiology for the radiologist. *Philadelphia, Pa. : Lippincott Williams & Wilkins*, 2006.

[5] B. Ehresmann et al. Charged particle spectra obtained with the Mars Science Laboratory Radiation Assessment Detector (MSL/RAD) on the surface of Mars. *Journal of Geophysical Research*, pages 468–479, 2014.

[6] C. G. Tate et al. Water equivalent hydrogen estimates from the first 200 sols of Curiositys traverse (Bradbury Landing to Yellowknife Bay): Results from the Dynamic Albedo of Neutrons (DAN) passive mode experiment. *Icarus*, pages 102–123, 2015.

[7] G. Gronoff et al. Computation of cosmic ray ionization and dose at mars. I: A comparison of HZETRN and planetocosmics for proton and alpha particles. *Space Research*, 55:7:1799–1805, 2015.

[8] Hassler et al. Mars' surface radiation environment measured with the mars science laboratory's curiosity rover. *Science*, 343(6169), 2013.

[9] P. Gonalves et al. Characterization of the particle radiation environment at three potential landing sites on mars using esas merem models. *Icarus*, 218:723–734, March 2011.

[10] P. Gonalves et al. Overview of energetic particle hazards during prospective manned missions to mars. *Planetary and Space Science*, 2011.

[11] Ralf Moeller et al. Astrobiological aspects of the mutagenesis of cosmic radiation on bacterial spores. *Astrobiology*, 10(5):509–521, June 2010.

[12] Ralf Moeller et al. Journal of the ICRU, vol 10 no 2. *Oxford University Press*, 2010.

[13] S. P. Swordy. The Energy Spectra and Anisotropies of Cosmic Rays. *Space Science Reviews*, 99:85–94, October 2001.